ELSEVIER

Materials Science and Engineering A270 (1999) 1–8

MATERIALS SCIENCE & ENGINEERING A

www.elsevier.com/locate/msea

The alloying effects of tantalum on the microstructure of an $\alpha_2 + \gamma$ titanium aluminide

D.J. Larson *, C.T. Liu, M.K. Miller

Oak Ridge National Laboratory, Metals and Ceramics Division, PO Box 2008, Oak Ridge, TN 37831-6376, USA

Received 12 September 1998; accepted 27 December 1998

Abstract

Atom probe field ion microscopy has been used to investigate the alloying effects of tantalum in a hot extruded two-phase ($\alpha_2 + \gamma$) Ti-47 at.% Al-2% Cr-1% Nb-0.80% Ta-0.20% W-0.15% B alloy in both stress-relieved (2 h at 900°C) and aged (2160 h at 800°C) conditions. Slightly over half of the tantalum additions were found to be in solution in the main matrix phases. The concentration of tantalum in the aged alloy was determined to be 0.43 ± 0.14% Ta and 0.47 ± 0.04% Ta in the α_2 and γ phases, respectively, indicating that tantalum does not partition strongly to either phase. The presence of tantalum does not reduce the strong oxygen partitioning to the α_2 phase, or modify the low boron concentrations measured in the α_2 and γ phases. However, the addition of tantalum does appear to change the most prevalent boride phase from MB_2 to MB and possibly to increase the rate at which near-equilibrium levels of Al and Ti are achieved in the α_2 and γ phases. In addition, tantalum appears be responsible for the precipitation of a $Ti(Cr, Al)_2$ phase which contains significant amounts of Ti, Al, Cr, Ta and W. © 1999 Elsevier Science S.A. All rights reserved.

Keywords: Titanium aluminides based on TiAl; Alloying effects; Tantalum; Titanium boride; Precipitates; Phase composition; Atom probe field ion microscopy

1. Introduction

Two-phase γ-based TiAl alloys are attractive for high temperature structural applications due to their low density and good strength at elevated temperatures. Recent work has focused on chemical alloying and thermomechanical processing in order to obtain a reasonable combination of elevated temperature strength and room temperature ductility in these materials [1,2]. Research has shown that small amounts of various ternary elements can improve the ductility of TiAl alloys. In addition, the formation of additional phases, such as the β phase, affects the mechanical properties of these materials [3–5].

The addition of tantalum to TiAl alloys has been investigated as a way to modify the deformation behavior, and research has shown a complex phase equilbria in the Ti–Al–Ta system [6–8]. Small tantalum additions (< 10%) to TiAl alloys containing 45–48% Al can modify the solidification behavior and solid-state transformations with respect to binary alloys [7]. In addition, tantalum can modify the interfacial structure and morphology of the α_2 phase and reduce the stacking fault energy [9]. On a more macroscopic scale, tantalum additions improve oxidation and creep resistance at elevated temperatures but increase the susceptibility of hot cracking ([1] and references within). Tantalum also improves the tensile ductility at ambient and elevated temperatures in hot extruded P/M TiAl alloys. Tantalum additions combined with tungsten additions are effective in grain refinement [10].

In order to understand the alloying effects of tantalum, it is essential to know the phase distribution and partitioning behavior of the elements present. Therefore, the goal of this research is to determine how the tantalum additions are distributed throughout the alloy (i.e. phase partitioning, interfacial segregation, etc.), if this distribution is strongly affected by annealing, and if the tantalum significantly modifies the behavior of other alloying additions. Atom probe field ion mi-

* Corresponding author. Tel.: +1-423-574-5357; fax: +1-423-574-0641.

E-mail address: larsondj@ornl.gov (D.J. Larson)

0921-5093/99/$ - see front matter © 1999 Elsevier Science S.A. All rights reserved.
PII: S0921-5093(99)00233-6

croscopy is a powerful tool with which to study elemental partitioning, precipitate composition and interfacial segregation because it can provide structural and chemical information about the microstructure of a material at the sub-nanometer level. In addition, because the atom probe is equally sensitive to all elements, it provides a means to investigate the behavior of light elements, such as boron, which cannot be easily examined using transmission electron microscopy with traditional energy dispersive spectrometry.

2. Experimental

The alloy investigated in this study had a nominal composition of Ti-47 at.% Al-2% Cr-1% Nb-0.80% Ta-0.20% W-0.15% B. The alloy powder was prepared by rapid solidification processing using the rotary atomization facility at Pratt and Whitney. The powder was canned and hot extruded at 1400°C (above T_α). After hot extrusion, alloy samples were stress-relieved for 2 h at 900°C and cooled in a vacuum furnace. Some samples of the alloy were also aged for 2160 h at 800°C in order to study the microstructural stability and alloying behavior in the material as it moved toward an equilibrium or near-equilibrium structure.

Field ion microscopy was performed with neon as the imaging gas. Atom probe analysis was performed in 1×10^{-7} Pa of Ne with a pulse fraction of 20% and a pulse repetition rate of 1500 Hz. The specimen temperature was 60 K for both field ion microscopy and atom probe analysis. All compositions are given in atomic percent and all composition error bars given are $\pm 2\sigma$.

3. Results and discussion

3.1. α_2 and γ Phases

The near fully-lamellar microstructure in the hot extruded alloy in the stress-relieved state was observed by optical microscopy, Fig. 1a. The yield strength and elongation of this material as a function of aging temperature is shown in Fig. 1b. Long term aging for 2160 h at 800°C does not produce significant changes in the optical microstructure. The lamellar microstructure in the stress-relieved and aged alloys was examined by field ion microscopy. The typical α_2/γ lamellar structure is shown in Fig. 2 for the stress-relieved sample.

The average compositions and the solute partitioning behavior of the α_2 and γ phases was measured in the atom probe and the results for both the stress-relieved and aged specimens are summarized in Tables 1 and 2. The aluminum concentration in the α_2 phase in the stress-relieved alloy was $30.5 \pm 1.23\%$ Al. In the aged alloy, the aluminum concentration in the α_2 phase was

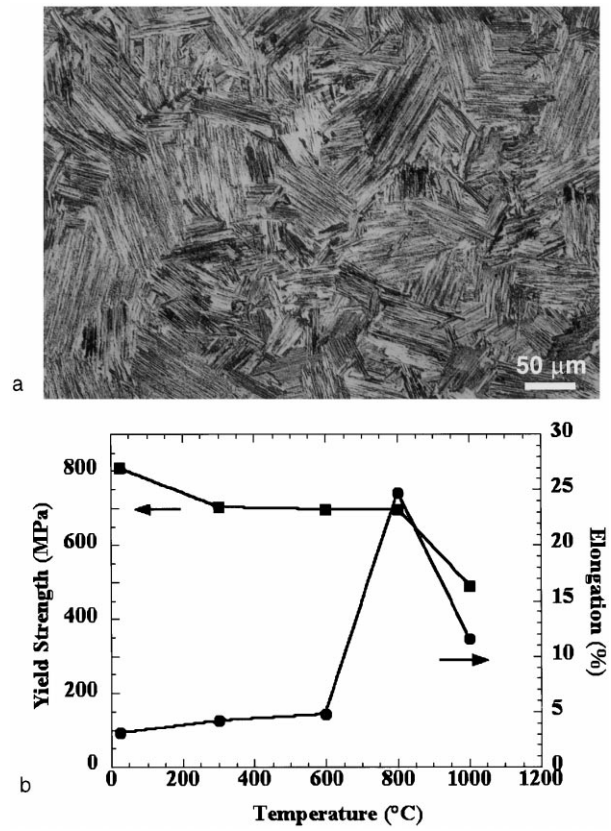

Fig. 1. (a) The optical microstructure and (b) tensile strength data for the stress-relieved alloy.

$30.4 \pm 0.96\%$ Al, indicating no significant change. Similarly, the titanium concentrations remain relatively constant upon aging. In previous investigations of a TiAl alloy without tantalum, aging for a shorter time of 720 h at 800°C produced significant changes in the Al and

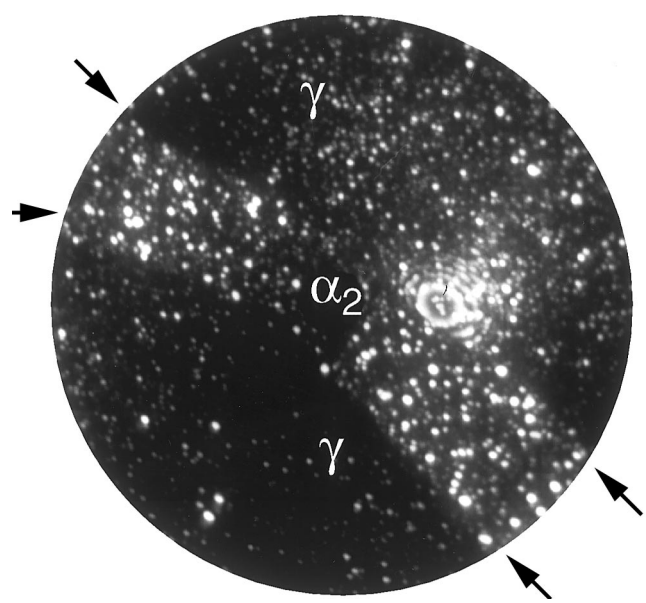

Fig. 2. Field ion image of α_2 and γ regions in the stress-relieved alloy.

Table 1
Matrix phase compositions for the stress-relieved and aged alloys

Phase	Heat treatment	Titanium	Aluminum	Chromium	Niobium	Tantalum	Oxygen	Tungsten	Boron
γ	2 h at 900°C	49.4 ± 0.36	46.8 ± 0.36	1.83 ± 0.10	1.02 ± 0.07	0.61 ± 0.06	0.07 ± 0.02	0.29 ± 0.03	0.014 ± 0.008
α_2	2 h at 900°C	62.0 ± 1.29	30.5 ± 1.23	2.17 ± 0.39	1.00 ± 0.27	0.80 ± 0.24	2.54 ± 0.42	0.43 ± 0.17	0.07 ± 0.07
γ	2160 h at 800°C	49.6 ± 0.31	47.6 ± 0.31	1.14 ± 0.07	0.90 ± 0.06	0.47 ± 0.04	0.06 ± 0.02	0.27 ± 0.04	0.012 ± 0.007
α_2	2160 h at 800°C	61.4 ± 1.0	30.4 ± 0.96	2.27 ± 0.31	0.72 ± 0.18	0.43 ± 0.14	4.21 ± 0.42	0.45 ± 0.14	0.04 ± 0.04
$Ti(Cr, Al)_2$	2160 h at 800°C	20.9 ± 1.94	19.5 ± 1.89	43.1 ± 2.36	1.64 ± 0.61	12.2 ± 1.56	0.17 ± 0.20	2.44 ± 0.73	*
Nominal composition		Balance	47%	2%	1%	0.8%	–	0.2%	0.15%

* None detected.

Ti levels in the α_2 phase [11,12]. Thus, it appears that the 0.8% Ta addition is affecting the kinetics in this system. (It should be noted that the previously investigated alloy was also processed differently.)

In the stress-relieved alloy, the chromium was found to partition only slightly to the α_2 phase with a partitioning factor of ~ 1.2:1 (Table 2). Aging of the alloy resulted in an increase in the chromium partitioning to the α_2 phase (Table 2) but this is seen to be the result of a lower concentration in the γ phase, not an increase of the α_2 phase concentration (Table 1). The niobium did not exhibit a significant preference for either α_2 or γ phase in the stress-relieved or aged alloys (Table 2) in general agreement with previously determined niobium behavior in a TiAl alloy of similar overall composition in both stress-relieved [11] and aged states [12].

The results of Table 1 show possible tantalum partitioning to the α_2 phase in the stress-relieved alloy. A previous compositional measurement using analytical electron microscopy in an $\alpha_2 + \gamma$ TiAl alloy also suggested slight tantalum partitioning to the α_2 phase [13], although it should be noted that the previously studied alloy did not contain W and B. In this study, the tantalum present in the matrix phases is depleted below the nominal alloy composition (0.8% Ta), especially in the aged alloy, where the tantalum levels are 0.43 ± 0.14% Ta and 0.47 ± 0.04% Ta in the α_2 and γ phases, respectively. Some solid solution strengthening due to these levels of tantalum in the matrix phases might be expected. However, the yield strength of two-phase TiAl alloys is mainly controlled by the interlamellar spacing; as a result, a solid solution strengthening effect due to tantalum was not detected in this alloy [10].

The atom probe results indicate that tungsten partitions to the α_2 phase in the stress-relieved alloy (Table 1) with a partitioning factor of ~ 1.5:1 and this increases slightly with aging (Table 2). The average tungsten concentrations in the γ phase were slightly above the nominal alloy level (0.20% W) for both the stress-relieved and aged alloys with the 2σ error bar (based on counting statistics) showing a small deviation (Table 1). However, the standard deviation of the average concentrations indicates significant variation from one region to another even after aging. Tungsten concentrations in various γ phase regions varied from 0.19 to 0.37% and from 0.15 to 0.51% in the stress-relieved and aged alloys, respectively.

The tungsten concentrations in the α_2 phase were relatively constant between the stress-relieved and aged alloys, with both levels considerably above the nominal alloy composition. For the atom probe analyses of the γ phase, 0.29 ± 0.03% W and 0.27 ± 0.04% W were measured in the stress-relieved and aged alloys, respectively. The small error bars (2σ) on these measurements, together with the even higher tungsten concentrations from the α_2 phase, suggest that the actual amount of tungsten in this alloy is probably greater than the nominal alloy composition of 0.20% W.

In the current study, the oxygen was found to partition to the α_2 phase in the stress-relieved alloy with a partitioning factor of ~ 36:1 and this approximately doubles upon aging (Table 2). Previous studies have shown the preferential location of oxygen in the α_2 phase in TiAl alloys [11,12,14,15]. One proposed explanation for this is that octahedral intersticies exists in the α_2 phase that are surrounded by six titanium atoms but these interstices are not present in the γ phase [15]. This leads to preferential interstitials, including oxygen, in the α_2 phase. The presence of tantalum in both of the main matrix phases does not appear to alter this oxygen partitioning behavior.

The average boron concentrations in the γ and α_2 phases in both the stress-relieved and aged alloys (Table 1) were found to be significantly lower than the nominal alloy composition of 0.15% B. This observation is

Table 2
Elemental partitioning relative to the γ phase composition in the stress-relieved and aged alloys

Ratio	Heat treatment	Chromium	Niobium	Tantalum	Oxygen	Tungsten	Boron
α_2/γ	2 h at 900°C	1.19:1	1:1.02	1.31:1	36.3:1	1.48:1	5:1
α_2/γ	2160 h at 800°C	1.99:1	1:1.25	0.91:1	70.2:1	1.67:1	3.3:1
$Ti(Cr, Al)_2/\gamma$	2160 h at 800°C	37.8: 1	1.82:1	26.0:1	2.8:1	9.04:1	0

consistent with the precipitation of boride phases (see below) and previous results from an $\alpha_2+\gamma$ TiAl alloy with boron additions [16]. Due to the large error bars on the boron concentration measurements imposed by counting statistics (Table 1), the partitioning of boron between the phases cannot accurately be determined.

3.2. $Ti(Cr,Al)_2$ Phase

A third phase of different imaging behavior and composition from the γ and α_2 phases was found to be present in both the stress-relieved and aged samples. This phase had not been observed in the previous field ion microscopy studies of TiAl alloys. Field ion microscopy images of this phase in the aged alloy (Fig. 3) show that it images with bright contrast relative to both the γ and α_2 phases. The brightly-imaging behavior implies that this phase has a higher evaporation field, and likely a higher melting temperature, than the γ and α_2 phases. The phase appears to be plate-shaped although no information on the shape of the precipitate along the specimen axis was obtained. Due to the small spatial extent of the phase, the crystal structure was not obtainable by indexing the prominent poles in the field ion images. Another example of this phase in the aged alloy is shown in Fig. 4a. A composition profile from the α_2 phase into the third phase and then from the third phase into the γ matrix is shown in Fig. 4b. It is evident that this phase is highly enriched in chromium, tantalum and tungsten. The average of three different composition measurements of this phase in the aged alloy is given in Table 1. The chromium concentration of $43.1 \pm 2.36\%$ Cr is several times higher than that measured in previous observations of the β phase in TiAl-based alloys [3,17,18].

Although no diffraction data was obtained from this phase, the Cr/Ti ratio of ~ 2 suggests a $TiCr_2$-based Laves phase [19] containing considerable alloying additions. Assuming geometrical rules for site-occupancy in Laves phases, Ti, Nb, Ta, and W would be expected to occupy 'A' sites [20]. Placing Al and Cr on 'B' sites yields a stoichiometry near AB_2. This is agreement with recent work on the Ti–Al–Cr system [21], which shows Al substituting for Cr with a very high solubility in the $TiCr_2$ C14 phase. In addition to the chromium enrichment, the data given in Table 2 show the large enrichment of this phase relative to the γ phase for both Ta and W. Although it is difficult to accurately quantify the oxygen in this phase due to the counting statistics, the oxygen concentration is certainly closer to γ phase levels ($\sim 0.05\%$) than α_2 phase levels (~ 1–5%). This chromium-enriched phase was not observed in previous investigations of TiAl alloys containing no tantalum [11,12], which suggests that the tantalum addition stabilizes this phase.

3.3. Precipitation of boride phases

As noted above, the measured boron concentrations in both the α_2 and γ phases of the stress-relieved and aged alloys were well below the nominal alloy level (Table 1). This depletion was a result of the formation of several different types of boride precipitates. (In the stress-relieved alloy, borides were observed in ten of the 22 samples investigated. In addition, borides were seen in seven of the 17 aged alloy samples examined.) The size of the borides was usually larger than the field of view in the field ion image and thus their size can only be estimated as being at least 100–200 nm. Borides were analyzed in the stress-relieved alloy (MB, M_2B)

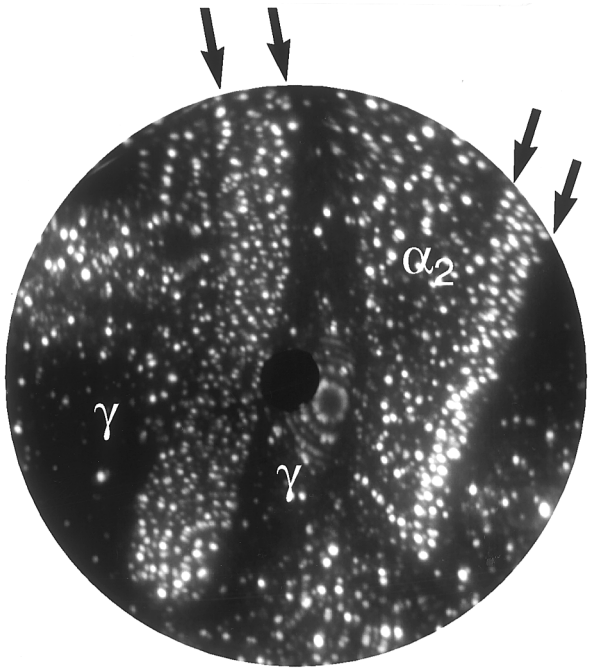

Fig. 3. Field ion images of two third-phase regions in contact with γ and α_2 regions in the aged alloy.

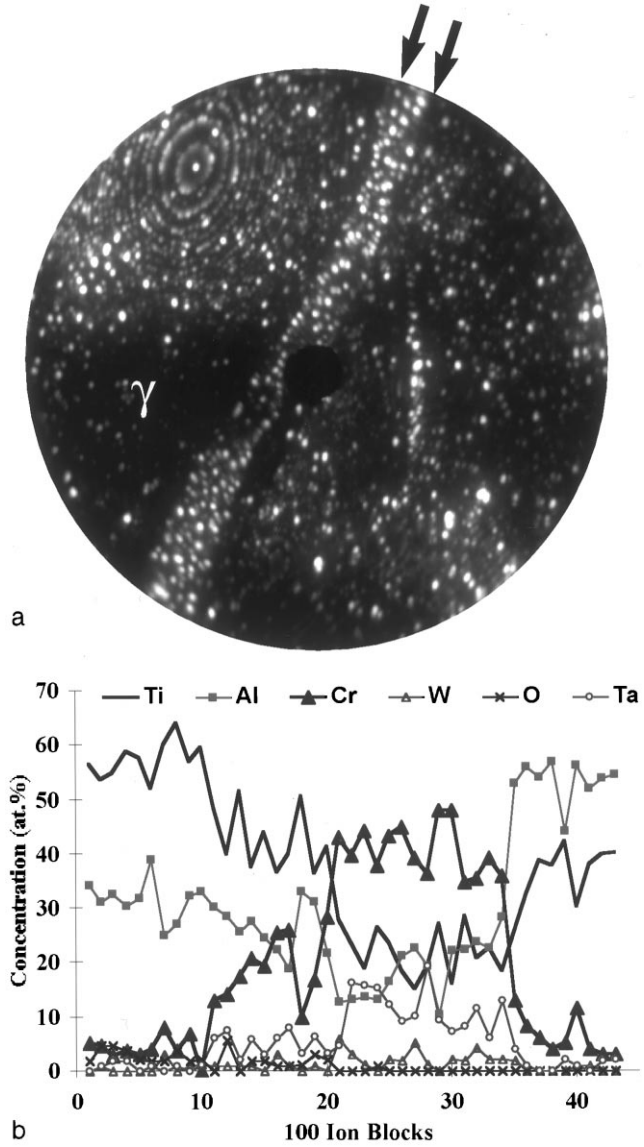

Fig. 4. (a) Field ion image and (b) corresponding composition profile through the third phase region in the aged alloy.

and in the aged alloy (MB and WB), Table 3. The MB phase was the most often detected phase in these alloys.

The metallic portion of the MB phase is primarily Ti (~ 73%) and Ta (~ 17%) with small amounts of W and Nb (where M denotes any combination of metallic elements). It is evident that the MB phase is slightly metal enriched, containing ~ 54% metallic species in the stress-relieved alloy.

Table 3
Boride compositions as determined by atom probe analysis

Heat treatment	Measured composition		Phase
Stress-relieved	$(Ti_{73.4}Nb_{4.5}Cr_{0.7}W_{4.4}Ta_{16.7}Al_{0.2})_{1.08}$	B	MB
Stress-relieved	$(Ti_{62.2}Nb_{2.4}Cr_{18.3}W_{4.3}Ta_{10.4}Al_{2.4})_{2.05}$	B	M_2B
Aged	$(Ti_{71.0}Nb_{5.4}Cr_{0.7}W_{6.9}Ta_{15.7}Al_{0.4})_{1.12}$	B	MB
Aged	$(Ti_{0.0}Nb_{11.8}Cr_{2.9}W_{83.8}Ta_{0.0}Al_{1.4})_{1.11}$	B	WB

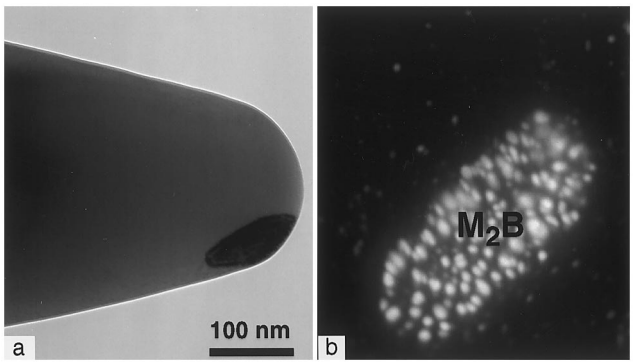

Fig. 5. (a) Field ion image and (b) transmission electron microscopy image of an M_2B boride in the stress-relieved alloy.

A chromium-enriched M_2B precipitate was detected and analyzed in the stress-relieved alloy (Table 3). This boride was significantly different in morphology relative to the more prevalent MB phase. Field ion and transmission electron microscopy images of this boride are shown in Fig. 5a and b, respectively. From these images it is evident that this boride is ~ 100 nm in diameter and roughly equiaxed in morphology. A boride phase of similar composition and morphology has been detected previously in an $\alpha_2 + \gamma$ TiAl alloy that did not contain tantalum [11,16].

Boride phases were also detected and analyzed in the aged alloy. As in the stress-relieved alloy, the MB phase was most prevalent. The metallic portion of the MB phase is primarily Ti (~ 71%) and Ta (~ 16%) with small amounts of W and Nb. The MB phase is metal enriched in the aged alloy, with the average boride containing ~ 56% M (Table 3). Another MB boride, which was sufficiently enriched in tungsten to be considered WB, was analyzed in the aged alloy (Table 3). The majority of the metallic portion of this phase consists of W (~ 84%) and Nb (~ 12%). This boride is also slightly metal rich, containing ~ 55% M (Table 3). It is of interest that this boride phase contains no tantalum.

No MB_2 phase was detected in either the stress-relieved or the annealed material. Thus it appears that the tantalum additions change the most prevalent boride phase from MB_2, as observed previously [11,16], to MB. This is in agreement with previous work by De Graf et al. [22] on TiAl alloys with Ta and B additions. It is also evident that a significant proportion of the alloying additions are contained in the borides (Table 3). No ultrafine boride precipitates (~ 10 nm diameter) were observed in either alloy during extensive field evaporation.

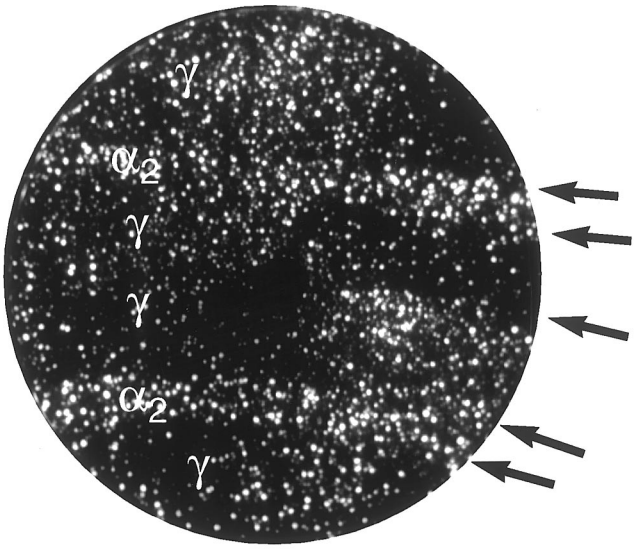

Fig. 6. Field ion image showing an α_2/γ interface in the stress-relieved alloy (analysis 1 in Table 4).

3.4. Segregation at interfaces

A preliminary investigation of interfacial segregation in the stress-relieved alloy was conducted. Two α_2/γ interfaces and one γ/γ interface were analyzed by atom probe. An α_2/γ interface in the stress-relieved alloy that was significantly enriched in chromium (3.41 ± 0.65% Cr) is shown in Fig. 6. The full composition from the interface is given as analysis 1 in Table 4. Despite the small diameter of the cylinder of analysis during this experiment (<4 nm), the data from the boundary analysis will contain a contribution from the matrix phases on either side of the interface. Thus, the actual segregation level at the interface is underestimated, and a geometric deconvolution procedure is necessary [23]. If the thickness of the interface region is assumed to be 0.23 nm (~ 1 atomic layer in the $\langle 111 \rangle$ direction), the coverage at the boundary is determined to be 11.1% Cr (Gibbsian interfacial excess of $\Gamma_i = 1.6 \times 10^{14}$ cm^{-2}). A coverage value of 0% corresponds to no segregation, i.e. the nominal alloy level of solute is present. There was no significant segregation of tungsten at this interface.

Atom probe analysis of another α_2/γ interface also revealed chromium enrichment at the interface (5.3 ± 2.3% Cr) with a coverage of 22.3% Cr ($\Gamma_i = 3.2 \times 10^{14}$ cm^{-2}). This boundary was analyzed by repositioning the probe aperture directly on the interface and at various distances on either side. A high oxygen concentration of the phase on one side of this interface confirmed the α_2 phase region. The full composition from the analyzed region directly on the boundary is given as analysis 2 in Table 4. The segregation of chromium to α_2/γ interfaces in the stress-relieved alloy is in agreement with previous atom probe results on TiAl alloys [11,12,24,25].

Field ion and transmission electron micrographs of a γ/γ interface in the stress-relieved alloy determined by atom probe to be enriched in Ta and possibly W (analysis 3 in Table 4) are shown in Fig. 7. Segregation of tungsten to α_2/γ and γ/γ interfaces in TiAl alloys has been reported previously [11,12,24] and is believed to be one of the factors responsible for resistance to growth and coarsening of the lamellar structures [2]. The coverage of tungsten at this boundary is calculated to be 1.4% ($\Gamma_i = 2.0 \times 10^{13}$ cm^{-2}). Note that there appears to be no chromium enrichment at this interface. Chromium segregation in polysynthetically twinned TiAl crystals has been observed by Inui et al. [26] at some γ/γ interfaces but not at others.

In a previous study [11,12], tungsten segregation was observed to be reduced after aging. Surprisingly, the tungsten segregation observed in the tantalum-containing material in the stress-relieved state correlates more closely with the previous results from the aged alloy, i.e. tungsten segregated to some, but not all, boundaries. This suggests that tantalum additions may assist in producing a faster approach to equilibrium in these alloys, consistent with observations given above deduced from the non-varying Al and Ti levels. Further work is required to confirm this behavior. The preliminary segregation results show no significant boron segregation at any of the interfaces analyzed, in agreement with investigations of interfaces in alloys of similar composition [11,12,16,24].

4. Summary

The following can be concluded regarding the additions of tantalum in TiAl alloys (note that the alloys were processed in different ways):

Table 4
Compositions from boundary regions in the stress-relieved alloy

Analysis	Heat treatment	Titanium	Aluminum	Chromium	Niobium	Tantalum	Oxygen	Tungsten	Boron
1	α_2/γ Interface	55.4 ± 1.78	37.1 ± 1.73	3.41 ± 0.65	1.13 ± 0.38	0.87 ± 0.33	1.35 ± 0.41	0.23 ± 0.17	*
2	α_2/γ Interface	52.4 ± 5.0	37.3 ± 4.86	5.29 ± 2.25	1.01 ± 1.0	1.26 ± 1.12	1.51 ± 1.22	0.76 ± 0.87	*
3	γ/γ Interface	50.6 ± 1.44	44.6 ± 1.43	2.0 ± 0.41	0.74 ± 0.25	1.32 ± 0.33	0.08 ± 0.08	0.39 ± 0.18	0.06 ± 0.07

* None detected.

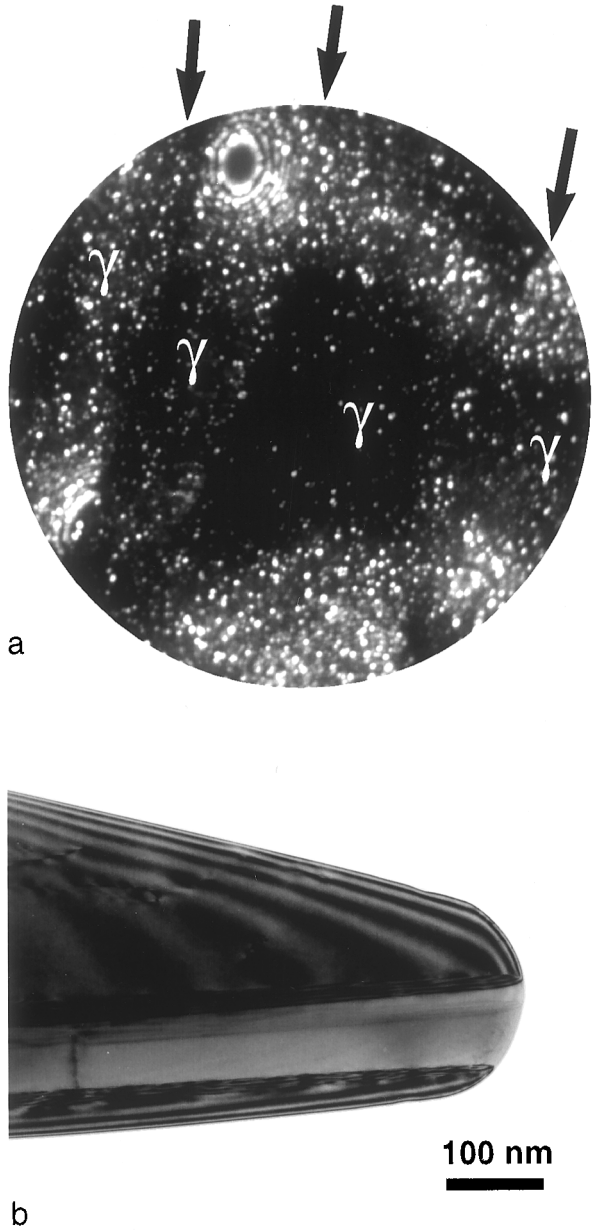

Fig. 7. (a) Field ion image and (b) transmission electron microscopy image of γ/γ interface in the stress-relieved alloy (analysis 3 in Table 4).

(1) The majority of the tantalum additions remain in solution in the α_2 and γ phases in the stress-relieved alloy, although a significant amount is present in the borides. Slightly greater than half of the tantalum additions remain in solution in the aged alloy.

(2) Tantalum changes the most prevalent boride phase from MB_2 to MB and produced a higher number density of borides.

(3) Tantalum appears to modify the kinetics of the system as manifested by little or no change in the Al and Ti concentration in the α_2 and γ phases between the stress-relieved and annealed states.

(4) Tantalum does not appear to affect the niobium behavior significantly.

(5) Tantalum does not modify the low boron solubility levels in the α_2 and γ phases or the strong partitioning of oxygen to the α_2 phase.

(6) Tantalum promotes precipitation of the $Ti(Cr,Al)_2$ phase which contains significant amounts of Ti, Al, Cr, Ta and W.

(7) Tantalum does not inhibit the segregation of chromium to interphase interfaces and may segregate itself.

Acknowledgements

The authors would like to thank K.F. Russell for technical assistance and Drs K.B. Alexander, I.M. Anderson, P.J. Maziasz, D.J. Thoma and M.L. Weaver for helpful comments. This research was sponsored by the Division of Materials Sciences, US Department of Energy, under contract DE-AC05-960R22464 with Lockheed Martin Energy Research Corp. and by an appointment (DJL) to the Oak Ridge National Laboratory (ORNL) Postdoctoral Research Associates Program administered jointly by the Oak Ridge Institute for Science and Education and ORNL. This research was conducted utilizing the Shared Research Equipment User Program facilities at ORNL.

References

[1] S.C. Huang, in: R. Darolia, J. Lewandowski, C.T. Liu, P. Martin, D. Miracle, M. Nathal (Eds.), Structural Intermetallics, TMS, Warrendale, PA, 1993, p. 299.
[2] P.J. Maziasz, R.V. Ramanujan, C.T. Liu, J.L. Wright, Intermetallics 5 (1997) 83.
[3] N. Masahashi, Y. Mizuhara, M. Matsuo, T. Hanamura, M. Kimura, K. Hashimoto, Iron Steel Inst. Jpn. Int. 31 (1991) 728.
[4] Y. Mizuhara, N. Masahashi, Scripta Metall. 27 (1992) 1079.
[5] M. Nobuki, D. Vanderschuren, M. Nakamura, Acta Metall. 42 (1994) 2623.
[6] S. Das, J.H. Perepezko, Scripta Metall. 25 (1991) 1193.
[7] C. McCullough, J.J. Valencia, C.G. Levi, R. Mechrabian, M. Maloney, R. Hecht, Acta Metall. 39 (1991) 2745.
[8] M.L. Weaver, M.J. Kaufman, Acta Metall. 43 (1995) 2625.
[9] S.R. Singh, J.M. Howe, Phil. Mag. A 66 (1992) 739.
[10] C.T. Liu, unpublished research.
[11] D.J. Larson, C.T. Liu, M.K. Miller, Mater. Sci. Eng. A 239–240 (1997) 220.
[12] D.J. Larson, M.K. Miller, Mater. Sci. Engr. A 250 (1998) 65.
[13] P.J. Maziasz, C.T. Liu, J.L. Wright, in: M.V. Nathal, R. Darolia, C.T. Liu, P.L. Martin, D.B. Miracle, R. Wagner, M. Yamaguchi (Eds.), Structural Intermetallics, TMS, Warrendale, PA, 1997, p. 245.
[14] R. Uemori, T. Hanamura, H. Morikawa, Scripta Metall. 26 (1992) 969.
[15] A. Menand, S. Huget, A. Nerac-Pertaix, Acta Mater. 44 (1996) 4729.
[16] D.J. Larson, C.T. Liu, M.K. Miller, Intermetallics 5 (1997) 411.
[17] S.C. Huang, E.L. Hall, Met. Trans. A 22 (1991) 2619.

[18] B. Zhang, J. Wang, X. Wan, W. Chen, Scripta Metall. 30 (1994) 399.
[19] J.D. Livingston, Phys. Stat. Sol (a) 131 (1992) 415.
[20] D.J. Thoma, private communication (1997).
[21] T.J. Jewett, M. Dahms, Z. Metallkd. 87 (1996) 254.
[22] M. De Graf, J.P.A. Löfvander, C.G. Levi, Acta Metall. 39 (1991) 2381.
[23] M.K. Miller, G.D.W. Smith, Appl. Surf Sci. 87/88 (1995) 243.
[24] D.J. Larson, C.T. Liu, M.K. Miller, Intermetallics 5 (1997) 479.
[25] A. Menand, H. Zapolsky-Tatarenko, A. Nerac-Pertaix, Mater. Sci. Engr. A 250 (1998) 55.
[26] H. Inui, K. Kishida, M. Kobayashi, M. Yamaguchi, M. Kawasaki, K. Ibe, Phil. Mag. A 74 (1996) 451.